THE JOURNAL OF PHYSICAL CHEMISTRY B LETTERS

2005, *109,* 21492−21495
Published on Web 10/27/2005

Electron Transport Across the Alkanethiol Self-assembled Monolayer/Au(111) Interface: Role of the Chemical Anchor

C. D. Lindstrom, M. Muntwiler, and X.-Y. Zhu*

Department of Chemistry, University of Minnesota, Minneapolis, Minnesota 55455

Received: August 18, 2005; In Final Form: October 11, 2005

Alkanethiol self-assembled monolayers (SAMs) on Au(111) are model systems for molecular electronics. We probe the role of the chemisorption bond on electron dynamics at the SAM/Au interface using time-resolved two-photon photoemission. Formation of the Au−S bond is evidenced by a localized σ^* resonance, which broadens and shifts upward in energy when the lying-down chemisorbed molecules stand up. The localized chemisorption bond does not affect the electronic coupling between delocalized image resonances and the metal substrate. Instead, lifetimes of image resonances are decreased due to scattering with S atoms within the thiol or thiolate monolayer.

Thiol self-assembled monolayers (SAMs) on metal surfaces, particularly Au(111), have served as models in the majority of recent studies on molecular electronics.[1] Among the SAM systems, alkanethiols on Au(111) are the most extensively studied.[2−4] It is known that the adsorption of alkanethiols [CH_3−$(CH_2)_n$−SH] from the vapor phase to form alkanethiolates [CH_3−$(CH_2)_n$−S−] on Au(111) at room temperature occurs in several steps.[3−5] At low coverage, adsorbed thiolates form a two-dimensional gas phase. As the surface concentration of thiolates increases, they nucleate into the lying-down "stripe-phase" with the long molecular axis parallel to the surface. When surface coverage further increases to near saturation, the thiolates stand-up to form the commensurate c(4×2) SAM phase. If the surface temperature is sufficiently low ($\leq$ 200 K), alkanethiols can physisorb on Au(111) to form molecular films with the thiol group (−SH) intact and with the long molecular axis parallel to the surface.[6] A key question of interest to molecular electronics is: how do changes in film structure and interfacial bonding affect electronic properties?

We probe this question using two photon-photoemission (2PPE) spectroscopy and the model system of hexanethiol/Au(111) in three forms: physisorbed hexanethiol monolayer, chemisorbed stripe-phase (lying-down) of hexanethiolates, and chemisorbed SAM-phase (standing-up) of hexanethiolates. 2PPE has been successfully applied as a probe of unoccupied states/resonances on metal surfaces and at metal−molecule interfaces.[7−10] The measurement can be carried out in time- and angle-resolved modes for the determination of the lifetime and parallel dispersion of the nominally unoccupied state. A particularly prevalent type of unoccupied states on metal surfaces are image states formed between the image barrier present on the vacuum side and the projected bulk band gap present on some metal surfaces.[7−11] These states possess free-electron like dispersion parallel to the surface and have a maximum binding energy relative to the vacuum level of 0.85 eV.[7−11] In the case of Au(111), there is no projected bulk-band gap in this energetic region, so these states become resonances that can decay via resonant electron transfer to the metal. A previous study showed that image resonances persist when *n*-alkanes are physisorbed on Au(111) and their lifetimes increase dramatically with increasing thickness of the molecular film.[12] This result serves as a reference point when we probe hexanethiols and hexanethioates on Au(111).

All experiments were carried out in an ultrahigh vacuum chamber detailed elsewhere.[12] Clean Au(111) was prepared by standard procedures.[12] 1-Hexanethiol ($C_6H_{13}SH$, 97%, Aldrich) was purified by freeze−pump−thaw cycles and the purity checked by a mass spectrometer. The gas exposure is reported in Langmuirs (1 L = 10^{-6} Torr·s). The physisorbed monolayer, deposited with the substrate at 90 K with an exposure of approximately 1 L, was verified by thermal desorption spectroscopy.[6] The striped, lying down phase of hexanethiolate was created by exposing the substrate at room temperature to ~30 L of hexanethiol.[5] The standing-up SAM phase was formed by a total dose of $\sim 1 \times 10^4$ L with the substrate held at room temperature.[3,5] Laser light for 2PPE (from a tunable Ti:sapphire oscillator) was split into two beams; one was frequency tripled to obtain photon energies from 4 to 5 eV (pump); the other (probe) passed through a delay stage and recombined with the pump beam. The recombined pump and probe beams were focused at the sample surface by an $f = 1$ m focusing mirror. Autocorrelation measurements of the IR probe beam on an interferometric autocorrelator showed that the laser pulses are of nearly transform-limited Gaussian shape (pulse width ~80 fs). Cross-correlation of the pump and probe pulses was used to determine the UV pulse width (~90 fs) based on 2PPE signal from the occupied surface state of clean Au(111). Monochromatic measurements were performed using the pump beam only. Photoelectrons were detected on a hemispherical electron energy analyzer (Vacuum Generators 100AX) with an instrumental resolution of 35 meV. The sample could be rotated to vary the angle of electron detection. Except for the angle-resolved

* To whom correspondence should be addressed. E-mail: zhu@chem.umn.edu; phone: (612) 624-7849; fax: (612) 625-0079.

10.1021/jp054663k CCC: $30.25

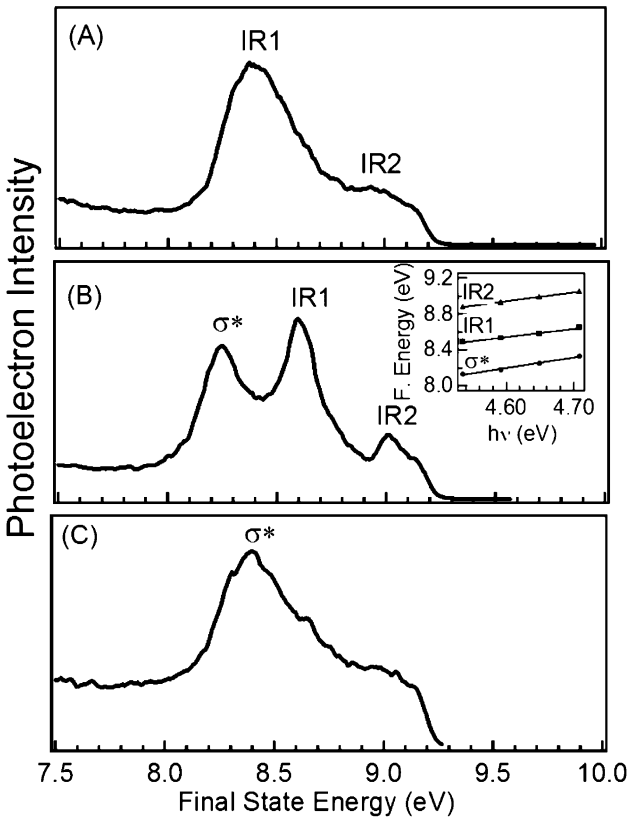

Figure 1. Monochromatic 2PPE spectra taken at $h\nu = 4.59$ eV for (A) physisorbed monolayer; (B) chemisorbed lying-down phase; and (C) chemisorbed standing-up phase of n-hexanethiol on Au(111). The inset shows $h\nu$ dependence of the final state energy for the three resonances in spectrum (B); the solid lines are linear fits with slopes of 1.0 ± 0.1. The final state energy is referenced to the Fermi level.

TABLE 1: Binding Energies (relative the vacuum level) of Unoccupied Resonances and Surface Workfunction for the Different Phases of *n*-Hexanethiol on Au(111)

feature	IR1 (eV)	IR2 (eV)	σ^* (eV)	work function
clean Au(111) [ref 13]	0.86	0.21	N/A	5.55
physisorbed *n*-heptane [ref 12]	0.60	0.15	N/A	4.90
physisorbed 1-hexanethiol	0.60	0.12	N/A	4.50
stripe-phase 1-hexanethiol	0.57	0.16	0.90	4.60
c(4 × 2) phase 1-hexanethiol	N/A	N/A	0.45	4.30

measurements, all other spectra were collected with the sample surface normal to the detector.

Figure 1 shows monochromatic (UV+UV) 2PPE spectra of (A) the physisorbed hexanethiol monolayer, (B) the chemisorbed stripe-phase hexanethiolate monolayer, and (C) the chemisorbed standing-up phase hexanethiolate SAM. The *x*-axis is final electron energy referenced to the Fermi level. All peaks correspond to unoccupied states transiently populated by the excitation photon; this is verified by the one-photon dependence of electron kinetic energy on photon energy in monochromatic measurements, as shown in the inset in Figure 1B for the stripe phase. The same conclusions are reached from analysis of the physisorbed phase and the standing-up SAM phase. Table 1 summarizes the binding energies (BE) of all the observed peaks for the three phases of hexanethiols on Au(111), along with those of image resonances on *n*-heptane/Au(111) and corresponding surface work functions. The assignment of these peaks is detailed below.

For the physisorbed monolayer, *n*-hexanethiol molecules lie flat on the Au(111) surface and its structure is expected to be

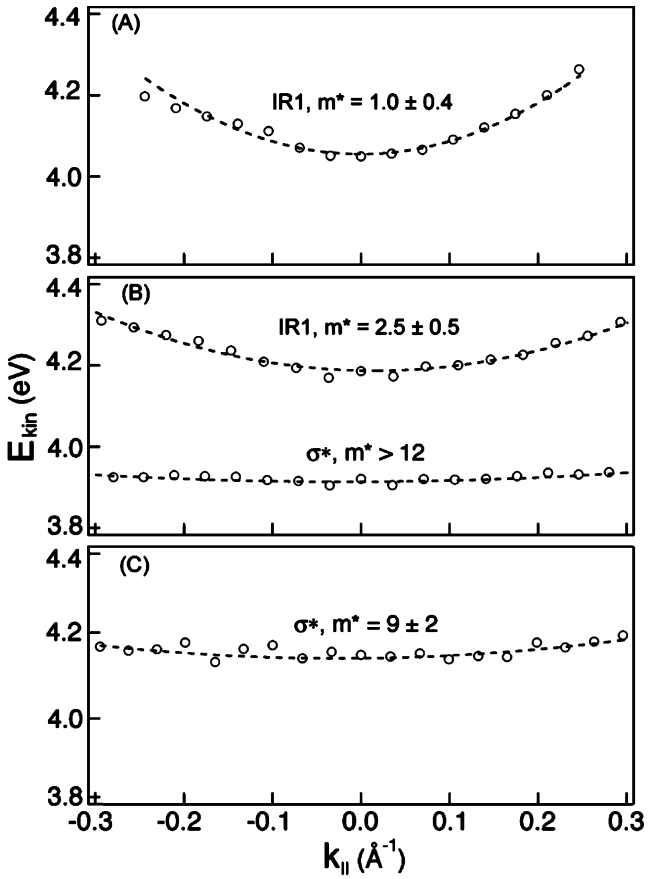

Figure 2. Parallel dispersions of the $n = 1$ image (IR1) and σ^* resonances from (A) physisorbed monolayer; (B) chemisorbed lying-down phase; and (C) chemisorbed standing-up phase of *n*-hexanethiol on Au(111). The dashed curves are parabolic fits to free electron like dispersion with the indicated effective electron masses (x m_e).

similar to that of *n*-alkanes on Au(111).[6,14] The two peaks in Figure 2a are assigned to the $n = 1$ and 2 image resonances (IR1 and IR2), as their binding energies are in excellent agreement with those of image resonances on monolayer *n*-heptane covered Au(111).[12] As expected for image resonances, parallel dispersions for the IR1 (Figure 2a) and IR2 peaks (data not shown) show free electron-like behavior, each with an effective electron mass equal to the free electron mass (m_e).

2PPE spectrum from the chemisorbed stripe phase (Figure 1b) shows two well-defined image resonance peaks, IR1 and IR2, in addition to a new peak σ^* (see below). The binding energies of the image resonances on the stripe phase are nearly the same as those on monolayer *n*-hexanethiol- or *n*-heptane-covered Au(111). This is understood as the thicknesses of the molecular layer and the dielectric constants are similar in all three cases. On the other hand, formation of the thiolate bond leads to an increase in the effective mass ($m_{eff} = 2.5$ m_e, Figure 2b) for the $n = 1$ image resonance, but not the $n = 2$ image resonance (data not shown). This is attributed to lateral corrugation of the electrostatic potential at the thiolate−Au interface, resulting in partial confinement of the electron wave function. Because the electron density in the $n = 2$ image resonance is spatially further away from the interface than that of $n = 1$, the corrugating potential at the interface has little effect. The corrugating potential can come from the transfer of a fraction of an electron upon S−Au bond formation,[15] along with polarization or charge redistribution of electron density near the adsorption site. For comparison, our recent study of the C_{60}/Cu(111) system showed complete localization of the *n*

$= 1$ image state by a much larger corrugating potential due to extensive electron transfer upon chemisorption (1.5−2 electron/molecule).[16]

In addition to image resonances, spectra from the chemisorbed stripe phase (Figure 2b) shows a new resonance (σ^*) located at 0.3 eV below the $n = 1$ image resonance. Angle-resolved measurement (Figure 2b) reveals little dispersion, indicating this unoccupied resonance is localized. Because it appears only after the formation of the chemisorption bond and because it is localized, we assign this resonance as the σ^* antibonding orbital for Au−S. This assignment follows prior studies of thiolates on Cu(111)[17] and methylthiolate on Ag(111).[18] Note that, referencing to the Fermi level, the σ^* resonance is located at 3.7 eV on Au(111), 3.3 eV on Cu(111), and 1.6 eV on Ag(111). It is not clear why the σ^* for the thiolate/Ag(111) interface is much lower than that on Au(111) or Cu(111). One possibility is the involvement of the d-band in S-metal bonding. The d-band is located at ∼2 eV below the Fermi level on Au or Cu; it is much deeper in energy on Ag, ∼4 eV below the Fermi level. This issue deserves further theoretical investigation.

When the thiolates stand up to form the SAM phase, Figure 1c, the image resonances are not clearly resolved and the spectrum is dominated by the σ^* peak. We assign this peak to the σ^* resonance because this peak shows negligible dispersion (Figure 2c) as compared to the image resonances. Since the σ^* resonance is observed for the chemisorbed stripe phase, it should also exist for the chemisorbed standing-up phase. Compared to the stripe phase, the σ^* resonance in the standing up phase broadens (full width at half-maximum increasing from ∼0.2 eV to ∼0.35 eV) and shifts up in energy (by 0.15 eV, referenced to the Fermi level). Both effects are expected from a stronger chemisorption bond as the alkyl group stands up; this reduces the strain of the S−Au thiolate bond. Note that, within experimental uncertainty, there is a very small but detectable dispersion of the σ^* resonance in the standing-up SAM phase. The solid curve in Figure 2c is fit to a free-electron-like dispersion with an effective electron mass of 9 m_e. Such a narrow band can be attributed to the small overlap of σ^* within the c(4 × 2) SAM structure. On the other hand, the S−Au bonds are much further apart spatially in the stripe phase and do not give rise to measurable dispersion. This observation is consistent with a study of Harris and co-workers, who measured the parallel dispersion of the σ^* state in methylthiolate on Ag(111).[18] They reported a low-density phase with no dispersion and a high-density phase with an effective electron mass as small as 0.5 m_e. The intermolecular distance in alkanethiolates on Ag(111) is shorter than that in the c(4 × 2) phase on Au(111).[2,4]

We determine the lifetimes of σ^* and image resonances from cross-correlation two color (UV pump + IR probe) 2PPE measurements. Coherent two photon ionization (UV + IR) of the occupied surface state on clean Au(111) is used as autocorrelation. Within experimental uncertainty, cross-correlations of the σ^* resonances and the $n = 1$ image resonance on the stripe phase covered surface are identical to that of the surface state, Figure 3a. This puts an upper limit of 20 fs on the lifetimes for IR1 and σ^*. The short lifetime of the σ^* resonance in the lying down or standing up phase is expected because it is strongly coupled to the metal substrate. Chemisorption resonances on metal surface usually possess widths from a fraction to a few eV or lifetimes on the order of a few femtoseconds.[7] However, the short lifetime ($\tau < 20$ fs) of the $n = 1$ image resonance on either the physisorbed hexanethiol monolayer or the stripe phase of chemisorbed hexanethiolate monolayer is unexpected. Because the thickness and the

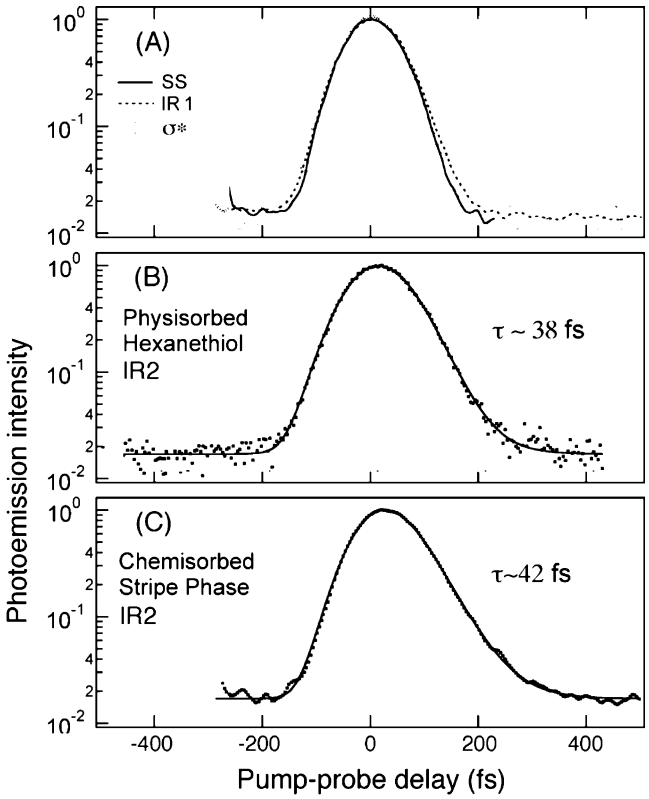

Figure 3. Pump−probe cross-correlations of (A) the $n = 1$ image resonance (dashed) and σ^* resonance (dots) from the stripe phase of *n*-hexanethiolates on Au(111); (B) the $n = 2$ image resonance on pyhsisorbed *n*-hexanethiol monolayer; and (C) the $n = 2$ image resonance on the stripe phase of *n*-hexanethiolate/Au(111). The solid curve in panel A is cross correlation from the occupied surface state on clean Au(111). The solid curves in panels B and C are fits based on rate equations[12] that give the indicated lifetimes.

dielectric constants of the physisorbed hexanethiol monolayer or the chemisorbed stripe phase are similar to those of *n*-heptane on Au(111), we would expect the lifetime of the $n = 1$ image resonance to be similar on all three surfaces. However, the $n = 1$ image resonance lifetime is $\tau = 54 \pm 10$ fs for physisorbed *n*-heptane monolayer on Au(111).[12] The substantial reduction (by at least a factor of 2−3) in this lifetime cannot be attributed to the formation of the chemisorption bond, because it is seen for both physisorbed thiol and chemisorbed thiolate phases. Instead, we attribute the reduced lifetimes to the presence of the S atom in the thiol or thiolate phases. A S atom is larger than the backbone C atoms, and there are occupied 3p orbitals in the former. The electrostatic potential introduced by these S atoms may serve as efficient scatters for an electron in the $n = 1$ image resonance, thus opening an additional decay channel. The presence of defects on clean metal surfaces is known to reduce image state lifetimes.[19]

Supporting this interpretation, we find that the lifetime of the n=2 image resonance is less affected. Lifetimes of the $n = 2$ image resonance on both the physisorbed hexanethiol monolayer (Figure 3B) and the chemisorbed stripe phase (Figure 3C) are measurable as the cross-correlation traces are broader than that of auto correlation. Fitting the data to a rate equation model including the so-called coherent artifact[20,21] or a three-level optical Bloch equation model[22,23] gives transient lifetimes of $\sim 40 \pm 10$ fs for the $n = 2$ image resonances on both surfaces. For comparison, lifetime of the $n = 2$ image resonance on the monolayer *n*-heptane/Au(111) surface is 65 ± 10 fs (data not shown). Going from the *n*-heptane monolayer to the physisorbed *n*-hexanethiol monolayer or the chemisorbed stripe phase of

n-hexanethiolate reduces the $n = 2$ image resonance lifetime by ~40%, much less than the change seen for $n = 1$. This is easily understood because the electron density in the $n = 2$ image resonance is further away from the interface than that in $n = 1$. For an ideal image state (i.e., hard wall potential at the surface and $1/4z$ image potential), the peaks in probability densities are at 2.2 and 11 Å from the surface for the $n = 1, 2$ image states. Thus, we expect much less scattering by the S atoms of an electron in the $n = 2$ resonance than that in the $n = 1$ resonance.

To conclude we find that, for *n*-hexanethiol SAMs on Au(111), formation of the chemisorption bond is characterized by a localized, σ^* antibonding resonance, which is strongly coupled to the metal substrate. The presence of the localized chemisorption bond does not increase the electronic coupling between delocalized image resonances and the metal substrate. The lifetime of the $n = 1$ image resonance on *n*-hexanethiol or *n*-hexanethiolate monolayer is reduced due to scattering by S atoms within the molecular film.

Acknowledgment. This work was supported by the National Science Foundation through grant CHE 0315165. Partial support from the National Science Foundation grant DMR 0238307 and the Swiss National Science Foundation in the form of a postdoctoral fellowship to M.M. is also acknowledged.

References and Notes

(1) Salomon, A.; Cahen, D.; Lindsay, S.; Tomfohr, J.; Engelkes, V. B.; Frisbie, C. D. *Adv. Mater.* **2003**, *15*, 1881.
(2) Ulman, A. *Chem. Rev.* **1996**, *96*, 1533.
(3) Poirier, G. E. *Chem. Rev.* **1997**, *97*, 1117.
(4) Schreiber, F. *Prog. Surf. Sci.* **2000**, *65*, 151.
(5) Kondoh, H.; Kodama, C.; Sumida, H.; Nozoye, H. *J. Chem. Phys.* **1999**, *111*, 1175.
(6) Lavrich, D. J.; Wetterer, S. M.; Bernasek, S. L.; Scoles, G. *J. Phys. Chem. B* **1998**, *102*, 3456.
(7) Harris, C. B.; Ge, N.-H.; Lingle, R. L., Jr.; McNeill, J. D.; Wong, C. M. *Annu. Rev. Phys. Chem.* **1997**, *48*, 711.
(8) Zhu, X.-Y. *Surf. Sci. Rep.* **2004**, *56*, 1.
(9) Machado, M.; Chulkov, E. V.; Silkin, V. M.; Höfer, U.; Echenique, P. M. *Prog. Surf. Sci.* **2004**, *17*, 219.
(10) Fauster, Th.; Reuss, C.; Shumay, I. L.; Weinelt, M. *Chem. Phys.* **2000**, *251*, 111.
(11) Echenique, P. M.; Pendry, J. B. *Prog. Surf. Sci.* **1990**, *32*, 111.
(12) Lindstrom, C. D.; Quinn, D.; Zhu, X.-Y. *J. Chem. Phys.* **2005**, *122*, 124714.
(13) Reuss, C.; Wallauer, W.; Fauster, Th. *Surf. Rev. Lett.* **1996**, *3*, 1547.
(14) Yourdshahyan, Y.; Rappe, A. M. *J. Chem. Phys.* **2002**, *117*, 825.
(15) Alloway, D. M.; Hofmann, M.; Smith, D. L.; Gruhn, N. E.; Graham, A. L.; Colorado, R., Jr.; Wysocki, V. H.; Lee, T. R.; Lee, P. A.; Armstrong, N. R. *J. Phys. Chem. B* **2003**, *107*, 11690.
(16) Dutton, G.; Pu, J.; Truhlar, D. G.; Zhu, X.-Y. J. *Chem. Phys.* **2003**, *118*, 4337.
(17) Vondrak, T.; Wang, H.; Winget, P.; Cramer, C. J.; Zhu, X.-Y. *J. Am. Chem. Soc.* **2000**, *122* 4700.
(18) Miller, A. D.; Gaffney, K. J.; Liu, S. H.; Szymanski, P.; Garret-Roe, S.; Wong, C. M. *J. Phys. Chem. A* **2002**, *106*, 7636.
(19) Fauster, T. *Surf. Sci.* **2002**, *507−510*, 256.
(20) Ogawa, S.; Petek, H. *Surf. Sci.* **1996**, *357−358*, 585.
(21) Knoesel, E.; Hotzel, A.; Wolf, M. *Phys. Rev. B* **1998**, *57*, 12812.
(22) Hertel, T.; Knoesel, E.; Hotzel, A.; Wolf, M.; Ertl, G. *J. Vac. Sci. Technol. A* **1997**, *15*, 1503.
(23) Boger, K.; Roth, M.; Weinelt, M.; Fauster, T. *Phys. Rev. B* **2002**, *65*, 075104.